RSC Advances

PAPER

View Article Online
View Journal | View Issue

Cite this: *RSC Adv.*, 2025, **15**, 29864

Synthesis, evaluation of *in vitro* cytotoxic activity, and *in silico* studies of some 3-methylenamino-4(3*H*)-quinazolone derivatives

Tuyen Ngoc Truong,[a] Em Canh Pham,[ab] Ngoc-Vi Nguyen Tran,[c] Phu Thien Tieu,[a] My Hanh Thi Cao,[a] Tuoi Thi Hong Do[a] and Khanh N. B. Le*[a]

A series of 3-methylenamino-4(3*H*)-quinazolone derivatives were synthesized by imine formation reactions of 3-amino-6-chloro-2-phenyl-4(3*H*)-quinazolone with various substituted aromatic aldehydes at 80 °C for 1–3 hours using the reflux method. Twenty 3-methylenamino-4(3*H*)-quinazolone derivatives were synthesized with good to excellent yields (66 to 90%). Compound **5** (2-chloro-6-fluorobenzylidene) exhibited good cytotoxic activity against the RD cell line with an IC_{50} value of 14.65 μM but exhibited weak cytotoxic activity against the MDA-MB-231 cell line (IC_{50} = 147.70 μM) compared to the reference drug paclitaxel (PTX, IC_{50} RD = 0.58 μM and IC_{50} MDA-MB-231 = 0.04 μM). Meanwhile, compounds **6** (benzo[*d*][1,3]dioxol-5-ylmethylene) and **7** (4-bromo-2-hydroxybenzylidene) showed good cytotoxic activity against MDA-MB-231 with IC_{50} values of 10.62 and 8.79 μM, respectively. However, these compounds showed weak cytotoxic activity against the RD cell line (IC_{50} = 50–55 μM). In particular, potential compounds **5**, **6**, and **7** exhibited weak cytotoxic activity against the normal cell line LLC-PK1 (IC_{50} = 34.82–60.18 μM) compared to the highly toxic agent PTX (IC_{50} = 1.31 μM). Furthermore, compounds **5**, **6**, and **7** showed strong interactions with the EGFR target with binding affinities of −9.6, −10.1, and −9.8 kcal mol^{-1}, respectively, compared to reference drug Gefitinib (−7.8 kcal mol^{-1}). The *in silico* ADMET results suggested that these potent derivatives possess a good ADMET profile. Therefore, these three compounds are potential candidates for novel cancer drug development, as demonstrated by *in vitro* and *in silico* studies.

Received 3rd June 2025
Accepted 31st July 2025

DOI: 10.1039/d5ra03933a

rsc.li/rsc-advances

1. Introduction

Heterocycles play a very important role in new drug development.[1–5] Quinazoline (or 1,3-diazanaphthalene/benzo[*d*]pyrimidine) is a double cyclic compound consisting of a pyrimidine ring condensed at position 5, 6 with a benzene ring. This scaffold is the pharmacophore nucleus present in many compounds with potential pharmacological effects, widely used in the pharmaceutical field.[1] Among quinazoline derivatives, the group of 4(3*H*)-quinazolone derivatives (or 4(3*H*)-quinazolinone) has received the most research attention, with many potential compounds having been synthesized and tested for biological activity.[2] Many studies have demonstrated that the quinazolone nucleus has diverse biological activities, such as antibacterial,[6–8] antifungal,[9] anticancer,[10–15] analgesic,[16–18] anti-inflammatory,[16,18] antiviral,[19,20] antituberculosis,[21] antioxidant,[22,23] and antihypertensive.[24] In particular, many 4(3*H*)-quinazolone derivatives have been developed into therapeutic drugs such as febrifugine (antimalarial), albaconazole (antifungal), balaglitazone (antihyperglycemic), diproqualone (GABAergic), afloqualone (GABAergic), fenquizone (diuretic), quinethazone (antihypertensive), halofuginone (antiprotozoal), and raltitrexed (anticancer) (Fig. 1).

In many research works, scientists have made efforts to improve the reactions to form 4(3*H*)-quinazolone heterocycles to evaluate or screen biological activities and discover active mechanisms. Many derivatives have shown potent anticancer properties.[25–34] In addition, the 4(3*H*)-quinazolone nucleus has many sites that can attach different substituents, especially at positions 2, 3, 6, and 7, from which many new derivatives with good biological effects can be created.[25–34] Moreover, the *N*-methylenamino substituent at position 3 can increase the anticancer activity of 4(3*H*)-quinazolone derivatives (Fig. 2).[12,15] However, research on 4(3*H*)-quinazolone derivatives with different substituents at position 3 (different *N*-methylenamino groups/N–N=C–R), 6-chloro, and 2-phenyl group is still limited, especially in terms of anticancer activity. Therefore, the study aimed to synthesize 3-arylmethylenamino-2-phenyl-4(3*H*)-quinazolone derivatives for anticancer activity screening, as well as molecular docking and *in silico* ADMET studies of potential active derivatives to create a scientific basis for the development of new cancer drugs.

[a]*School of Pharmacy, University of Medicine and Pharmacy at Ho Chi Minh City, Ho Chi Minh City, 700000, Vietnam. E-mail: lnbkhanh@ump.edu.vn*

[b]*Faculty of Pharmacy, Hong Bang International University, Ho Chi Minh City, 700000, Vietnam*

[c]*Faculty of Pharmacy, Uppsala University, Uppsala, 75105, Sweden*

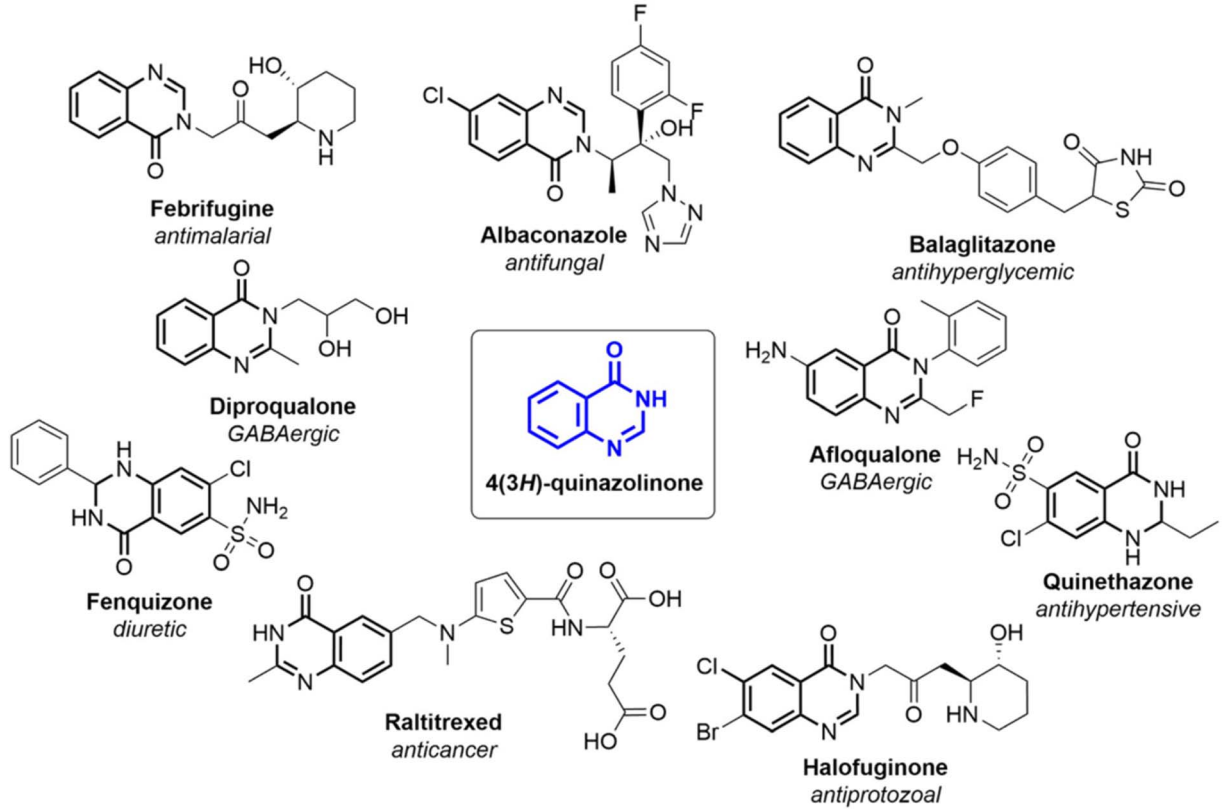

Fig. 1 Drugs containing 4(3*H*)-quinazolone nucleus.

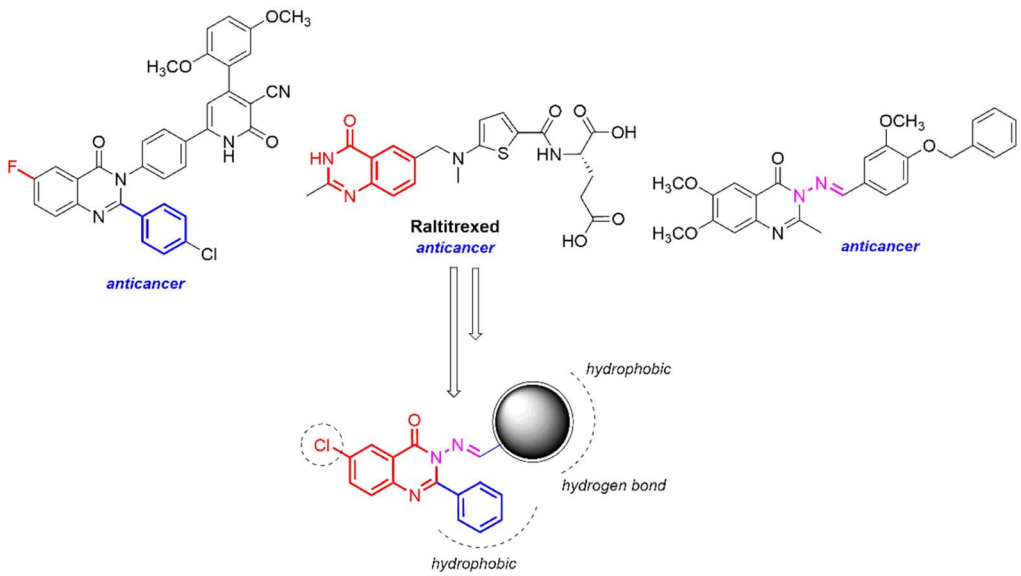

Fig. 2 Rational drug design of potential anticancer 4(3*H*)-quinazolone derivatives.

2. Results and discussion

2.1 Chemistry

The first step of the procedure involved dehydration and cyclization using 5-chloroanthranilic acid and benzoyl chloride as starting materials. Our effort resulted in a relatively simple procedure with a high yield of 85%. Notably, this stage requires an anhydrous environment and precise temperature control. Due to the moisture-sensitive nature of benzoyl chloride, anhydrous pyridine obtained by distillation was chosen as the solvent. This exothermic reaction generates the temperature-sensitive 4*H*-benzo[*d*][1,3]-oxazin-4-one (**Q0**), which demands

Table 1 Yields and reaction times of 3-methylenamino-4(3*H*)-quinazolone derivatives

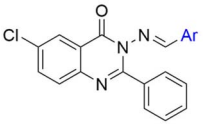

Code	Ar-group	Compound	Yield	Reaction time (h)
1	—	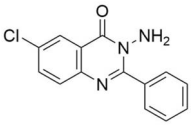	66	2.0
2	4-Nitrophenyl	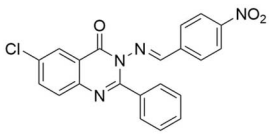	68	2.0
3	3,4-Dichlorophenyl	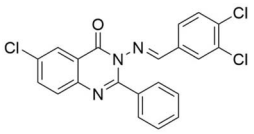	85	1.5
4	4-Fluorophenyl	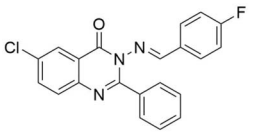	85	1.5
5	2-Chloro-6-fluorophenyl	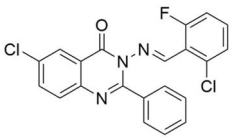	86	1.0
6	Benzo[*d*][1,3]dioxol-5-yl	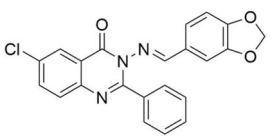	72	2.0
7	4-Bromo-2-hydroxyphenyl	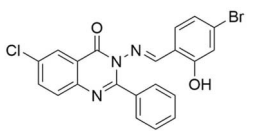	88	1.0
8	4-(Dimethylamino)phenyl	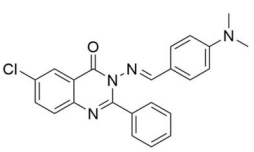	90	1.0
9	3-Hydroxyphenyl	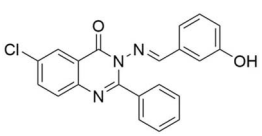	81	1.5
10	4-Ethoxy-3-hydroxyphenyl	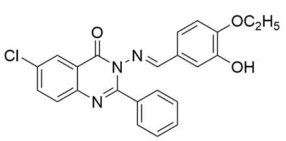	87	1.0

Table 1 (*Contd.*)

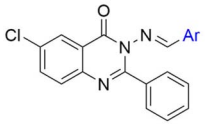

Code	Ar-group	Compound	Yield	Reaction time (h)
11	2,4-Dichlorophenyl	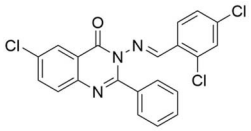	85	1.0
12	2-Chlorophenyl	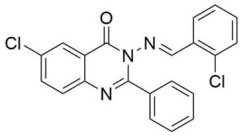	82	1.5
13	3,4-Dimethoxyphenyl	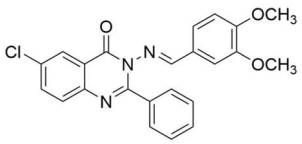	86	1.0
14	Pyridin-3-yl	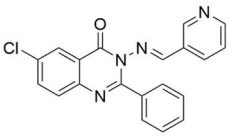	72	2.0
15	Furan-2-yl	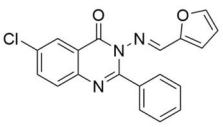	77	2.0
16	3-Nitrophenyl	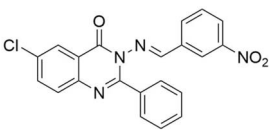	78	2.0
17	4-Ethoxyphenyl	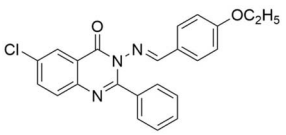	86	1.0
18	3-Methoxyphenyl	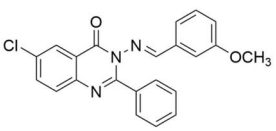	83	1.5
19	2-Hydroxyphenyl	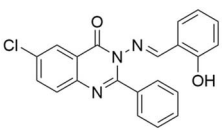	83	1.5
20	3-Hydroxy-4-methoxyphenyl	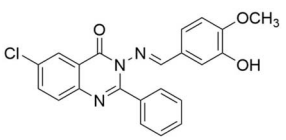	85	1.0

Table 1 (*Contd.*)

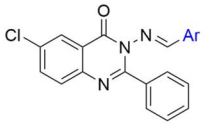

Code	Ar-group	Compound	Yield	Reaction time (h)
21	Phenyl	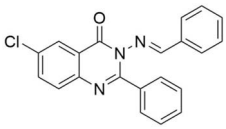	80	1.5

a low reaction temperature. Subsequently, purified **Q0** can only be dried under vacuum at a temperature below 40 °C.

In the second step, **Q0** reacts with hydrazine hydrate, in the presence of sulfuric acid and PPA as cyclization and dehydration catalysts, forming 3-amino-6-chloro-2-phenyl-4(3*H*)-quinazolone (**1**). The reaction proceeded for approximately 3–4 hours, yielding 66%. In other studies, the absence of 6-chloro substitution led to higher yields (around 88%), even in the absence of cyclization catalysts.[19] This suggests that the introduction of a 6-chloro substituent interferes with the cyclization process.

Finally, from 3-amino-6-chloro-2-phenyl-4(3*H*)-quinazolone (**1**), imine formation was carried out, yielding 20 derivatives (**2–21**) with good yields (66–90%) (Table 1). Imine formation is generally conducted in acidic solvents (glacial acetic acid, ethanol, *etc.*) (Scheme 1). Meanwhile, 3-amino-6-chloro-2-phenyl-4(3*H*)-quinazolone (**1**) is unstable in acidic aqueous solution at high temperatures. Attempts have been made to seek an appropriate condition to maintain the integrity of the quinazolinone ring while forming the imine derivatives. Absolute ethanol was selected as the solvent, and the reaction was done at 80 °C for 1–3 hours. The reaction time and yield depended on the type, number, and position of substituents on the phenyl ring. Higher yields and shorter reaction times were observed with derivatives containing electron-donating groups, two substituents, and *para*- or *ortho*-substitutions.

Spectra investigation by FT-IR, MS, ^{1}H NMR, and ^{13}C NMR has confirmed the molecular structure of the synthesized compounds **Q0**, **1–21**. Stretching frequency in FT-IR spectra within the region 3380–3450 cm^{-1} due to C=N was observed, and that between 1660–1692 cm^{-1} indicated C=O of quinazolinone. In several mass spectra, ion peaks with a relative ratio of 7 : 3 could be encountered, which are aligned with the presence of chlorine (^{35}Cl and ^{37}Cl in a ratio of 3 : 1) in all structures. Additionally, ion peaks of 274 *m*/*z* have been regularly seen in curated MS spectra. The structure with a molecular mass of 274 *m*/*z* was predicted as in Fig. 3, given that the C=N imine and N_3–C_4 bonds are less stable and more likely to cleave during the fragmentation.

2.2 *In vitro* cytotoxic activity

The IC_{50} results (μM) on two cancer cell lines (RD – rhabdomyosarcoma cell line and MDA-MB-231 – human breast cancer cell line) and one normal cell line (LLC-PK1 – pig kidney-derived cell line) are presented in Table 2. The comparison of IC_{50} values of the 3-methylenamino-4(3*H*)-quinazolone derivatives

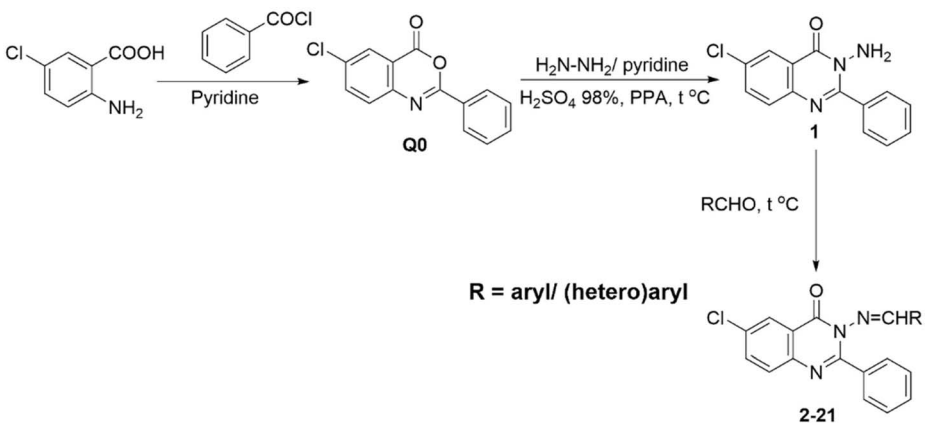

Scheme 1 Synthesis of 3-methylenamino-4(3*H*)-quinazolone derivatives (PPA: polyphosphoric acid).

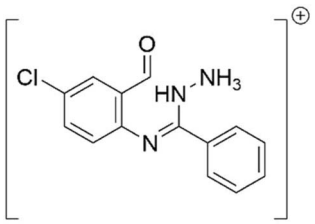

Fig. 3 Predicted structure depiction of the ion peak of 274 *m/z*.

with potential anticancer activity against the cancer cell lines RD, MDA-MB-231, and LLC-PK1 compared to the reference drug Paclitaxel (PTX) is shown in boldface.

Compounds **2–4** and **8–21** exhibited weak to moderate cytotoxic activity against two cancer cell lines RD (38.59–430.03 μM) and MDA-MB-231 (21.61–328.90 μM), compared to the reference drug PTX (IC_{50} RD = 0.58 μM and IC_{50} MDA-MB-231 = 0.04 μM). Compound **5** (2-chloro-6-fluorobenzylidene) exhibited good cytotoxic activity against RD with an IC_{50} value of 14.65 μM but exhibited weak cytotoxic activity against MDA-MB-231 with an IC_{50} value of 147.70 μM. In contrast, compounds **6** (benzo[*d*][1,3] dioxol-5-ylmethylene) and **7** (4-bromo-2-hydroxybenzylidene) showed good cytotoxic activity against MDA-MB-231 with IC_{50} values of 10.62 and 8.79 μM, respectively. However, these two compounds exhibited weak cytotoxic activity (IC_{50} = 50–55 μM) against the RD cell line. Notably, three potential compounds **5**, **6**, and **7** exhibited weak cytotoxic activity against the normal cell line LLC-PK1 (IC_{50} = 34.82–60.18 μM), while the reference drug PTX exhibited strong cytotoxicity against LLC-PK1 with an IC_{50} of 1.31 μM. These results showed that potential compounds **5**, **6**, and **7** showed selective cytotoxic activity on cancer cell lines. Therefore, these compounds are promising for further research for the development of new cancer therapeutic agents.

Several 6-substituted 4(3*H*)-quinazolone and chloro-4(3*H*)-quinazolone derivatives have been demonstrated to have potential cytotoxic activity. The 6-methyl-4(3*H*)-quinazolone derivative with 2-thio (amide) and 3-phenyl substituents showed IC_{50} values of approximately 20 μg mL^{-1} and exhibited stronger inhibitory activity against HT-29 (72%) and SW620 (63.3%) cell lines than fluorouracil (34.1% for HT-29 and 57.3% for SW620).[13] Meanwhile, the 6-methyl-4(3*H*)-quinazolone derivative with 2-thio (ester) and 3-(4-fluorophenyl) substituents exhibited strong cytotoxic activity against A549, MDA-MB231, and HeLa cell lines with IC_{50} values of 0.57, 1.19, and 1.26 mM, respectively.[14] In addition, the 7-chloro-4(3*H*)-quinazolone derivative showed antitumor activity against murine leukemia L-1210 cell line and human leukemia K-562 and HL-60 cell lines.[10] The 6-fluoro-4(3*H*)-quinazolone derivative with 2-methyl and 3-phenyl substituents showed potential antitumor activity against MCF-7 (IC_{50} = 3.42 μM) and NCI (IC_{50} = 2.51 μM) cell lines.[11] Furthermore, the 6-fluoro-4(3*H*)-quinazolone derivative with a 2,3-diphenyl substituent showed potential antitumor activity with high percentage inhibition against MCF-7 (97.5%) and HepG2 (94.6%) cell lines at a concentration of 25 μmol for 48 h.[12] The present study also demonstrated that 6-chloro-4(3*H*)-quinazolone derivatives have good and selective anticancer activity. The attachment of small substituents (halogen) at position 6 and large substituents (aromatic) at position 3 in the 4(3*H*)-quinazolone scaffold may be responsible for the potential and selective anticancer activity of these derivatives.

Table 2 Anticancer activity of 3-methylenamino-4(3*H*)-quinazolone derivatives (IC_{50}, μM)[a]

Entry	Compound	RD	MDA-MB-231	LLC-PK1
1	**2**	151.23 ± 2.06	104.33 ± 3.63	114.73 ± 9.50
2	**3**	246.33 ± 24.26	91.50 ± 1.47	336.70 ± 24.67
3	**4**	235.20 ± 8.29	21.61 ± 1.11	86.66 ± 1.95
4	**5**	**14.65 ± 0.68**	147.70 ± 5.64	**46.39 ± 2.06**
5	**6**	54.48 ± 0.81	**10.62 ± 0.67**	**60.18 ± 1.17**
6	**7**	51.61 ± 1.19	**8.79 ± 0.34**	**34.82 ± 0.27**
7	**8**	198.43 ± 18.90	100.80 ± 3.75	62.84 ± 3.67
8	**9**	253.53 ± 14.23	84.41 ± 1.26	320.93 ± 4.31
9	**10**	430.03 ± 72.90	85.55 ± 2.32	341.50 ± 29.25
10	**11**	251.30 ± 25.50	99.44 ± 1.76	264.33 ± 31.89
11	**12**	126.43 ± 6.20	321.47 ± 51.82	350.53 ± 56.08
12	**13**	129.53 ± 10.39	138.90 ± 4.04	461.73 ± 49.45
13	**14**	135.73 ± 16.98	262.07 ± 43.92	326.47 ± 18.18
14	**15**	38.59 ± 1.07	56.60 ± 5.37	154.37 ± 3.54
15	**16**	82.33 ± 1.99	300.77 ± 27.11	148.97 ± 5.50
16	**17**	376.23 ± 8.08	194.50 ± 8.83	136.17 ± 8.14
17	**18**	84.81 ± 9.35	328.90 ± 47.24	176.87 ± 3.22
18	**19**	51.09 ± 0.99	37.50 ± 0.63	75.70 ± 3.01
19	**20**	48.10 ± 3.97	198.27 ± 13.27	279.43 ± 29.14
20	**21**	142.57 ± 12.69	120.60 ± 9.35	302.90 ± 38.82
21	PTX	0.58 ± 0.01	0.04 ± 0.02	1.31 ± 0.05

[a] Mean ± SD, PTX – paclitaxel, RD – rhabdomyosarcoma cell line, MDA-MB-231 – human breast cancer cell line, LLC-PK1 – pig kidney-derived cell line.

2.3 *In silico* ADMET profile

Three potential compounds **5**, **6**, and **7** showed the physicochemical properties agreed with the directions of drug-likeness rules, including Lipinski (MW ≤ 500, MLOGP ≤ 4.15, *n*HA ≤ 10, and *n*HD ≤ 5), Veber (*n*Rot ≤ 10 and TPSA ≤ 140), and Egan (WLOGP ≤ 5.88 and TPSA ≤ 131.6), similar to reference drug Gefitinib (GEF), while reference drug paclitaxel (PTX) did not show agreement with all drug-likeness rules. In particular, compound **6** also exhibited physicochemical properties agreed with many drug-likeness rules such as Lipinski, Veber, Egan, Ghose (160 ≤ MW ≤ 480, −0.4 ≤ WLOGP ≤ 5.6, 40 ≤ MR ≤ 130, and 20 ≤ atoms ≤ 70), and Muegge (200 ≤ MW ≤ 600, −2 ≤ XLOGP ≤ 5, TPSA ≤ 150, num. Rings ≤ 7, num. Carbon > 4, num. Heteroatoms > 1, *n*Rot ≤ 15, *n*HA ≤ 10, and *n*HD ≤ 5) compared to GEF (Table 3).

In absorption, compounds **5**, **6**, and **7** showed good parameters, including Caco-2 permeability, MDCK permeability, PAMPA, Pgp-substrate, HIA (human absorption intestinal), $F_{20\%}$, $F_{30\%}$, and $F_{50\%}$, compared to PTX and GEF. Furthermore, the Caco-2 permeability of these compounds showed an excellent level (higher than −5.15 log unit), similar to GEF. The study results predicted that these compounds show high gastrointestinal absorption, accordingly, they may have remarkably good bioavailability after oral administration.

Table 3 ADMET profile of potential compounds and reference drugs

Parameter	5		6		7		PTX		GEF	
Physical chemistry										
Molecular weight (g mol^{-1})	412.24		403.82		454.70		853.91		446.90	
*n*HA	4		5		4		14		7	
*n*HD	0		0		1		4		1	
*n*Rot	3		3		3		15		8	
Log $P_{o/w}$ (XLOGP3)	5.52		4.61		5.13		3.66		4.11	
Log $P_{o/w}$ (WLOGP)	5.81		4.33		5.07		3.41		4.32	
Log $P_{o/w}$ (MLOGP)	5.58		4.24		4.75		1.7		2.82	
TPSA	47.25		65.71		67.48		221.29		68.74	
Log *S* (SILICOS-IT)	−8.96		−7.83		−8.30		−8.80		−7.94	
Solubility/H_2O (mg mL^{-1})	4.52×10^{-7}		6.04×10^{-6}		2.27×10^{-6}		1.34×10^{-6}		5.14×10^{-6}	
Molar refractivity	110.85		111.95		115.61		218.96		121.66	
Druglikeness										
Lipinski	Yes		Yes		Yes		No		Yes	
Ghose	No		Yes		Yes		No		Yes	
Veber	Yes		Yes		Yes		No		Yes	
Egan	Yes		Yes		Yes		No		Yes	
Muegge	No		Yes		No		No		Yes	
Bioavailability score	0.55		0.55		0.55		0.17		0.55	
Absorption										
Caco-2 permeability	−4.646	**E**	−4.871	**E**	−4.836	**E**	−5.904	**P**	−4.911	**E**
MDCK permeability	0	**E**	0	**E**	0	**E**	0	**E**	0	**E**
PAMPA	−−−	**E**	−−−	**E**	−−−	**E**	+++	**P**	++	**P**
Pgp-inhibitor	+++	**P**	+++	**P**	+++	**P**	−	**M**	−	**M**
Pgp-substrate	−−−	**E**	−−−	**E**	−−−	**E**	+++	**P**	+++	**P**[a]
HIA	−−−	**E**	−−−	**E**	−−−	**E**	−−−	**P**	−−−	**E**
$F_{20\%}$	−−−	**E**	−−−	**E**	−−−	**E**	++	**P**	−−−	**E**
$F_{30\%}$	−−−	**E**	−−−	**E**	−−−	**E**	+++	**P**	−−−	**E**
$F_{50\%}$	−−−	**E**	−	**E**	−−−	**E**	+++	**P**	−−−	**E**
Distribution										
PPB (%)	98.80	**P**	98.70	**P**	98.60	**P**	92.60	**P**	89.40	**E**
VDss (L kg^{-1})	0.71	**E**	0.969	**E**	0.995	**E**	1.025	**E**	2.565	**E**
BBB penetration	−	**M**	++	P	−−−	**E**	−−−	**E**	−−−	**E**
Fu (%)	0.70	**P**	0.90	**P**	1.00	**P**	7.00	**E**	10.50	**E**
OATP1B1 inhibitor	++	**P**	−	**M**	+	**M**	+++	**P**	+++	**P**
OATP1B3 inhibitor	++	**P**	+++	**P**	+++	**P**	+++	**P**	+++	**P**
BCRP inhibitor	−−−	**P**	−−−	**P**	−−−	**P**	−−−	**P**	+++	**P**
MRP1 inhibitor	−−−	**E**	−−−	**E**	−−−	**E**	+++	**P**	+++	**P**
BSEP inhibitor	+++	**P**	+++	**P**	+++	**P**	−	**P**	+++	**P**
Metabolism										
CYP1A2 inhibitor	+++		+++		+++		−−−		−	
CYP1A2 substrate	+++		+++		−−−		−−−		−	
CYP2C19 inhibitor	+++		+++		+++		−−−		−−−	
CYP2C19 substrate	−−−		−−−		−−−		−−−		+	
CYP2C9 inhibitor	+++		+++		+++		−−−		−−−	
CYP2C9 substrate	++		+++		−		−−−		−−−	
CYP2D6 inhibitor	−−−		+++		−		−−−		+++	
CYP2D6 substrate	−−−		−−		−−−		−−−		+++	
CYP3A4 inhibitor	−−−		+++		−−−		−−−		+	
CYP3A4 substrate	−−		−−−		−−−		+++		+++	
CYP2B6 inhibitor	−−−		+		−−		+++		−	
CYP2B6 substrate	−−−		−−−		−−−		−−−		−−−	
CYP2C8 inhibitor	+++		+++		+++		+++		+++	
HLM stability	−−−	**P**	−−−	**P**	−−	**P**	+	**M**	+++	**E**
Excretion										
CL_{plasma} (mL min^{-1} kg^{-1})	3.227	**E**	2.356	**E**	2.55	**E**	3.15	**E**	6.422	**M**
$T_{1/2}$	1.296		1.032		1.212		2.485		0.844	

Table 3 (*Contd.*)

Parameter	5		6		7		PTX		GEF	
Toxicity										
hERG blockers	0.315	**M**	0.404	**M**	0.031	**E**	0.022	**E**	0.899	**P**
hERG blockers (10 μm)	0.723	**P**	0.714	**P**	0.246	**E**	0.094	**E**	0.702	**P**
DILI	0.996	**P**	0.994	**P**	1	**P**	1	**P**	0.971	**P**
AMES toxicity	0.841	**P**	0.889	**P**	0.913	**P**	0.999	**P**	0.608	**M**
Rat oral acute toxicity	0.395	**M**	0.244	**E**	0.076	**E**	0.899	**P**	0.736	**P**
FDAMDD	0.789	**P**	0.893	**P**	0.945	**P**	0.998	**P**	0.647	**M**
Skin sensitization	0.896	**P**	0.931	**P**	0.985	**P**	1	**P**	0.458	**M**
Carcinogenicity	0.759	**P**	0.955	**P**	0.979	**P**	0.087	**E**	0.678	**M**
Eye corrosion	0	**E**	0	**E**	0	**E**	0	**E**	0	**E**
Eye irritation	0.361	**M**	0.363	**M**	0.976	**P**	0	**E**	0.152	**E**
Respiratory toxicity	0.825	**P**	0.67	**M**	0.099	**E**	0.11	**E**	0.77	**P**
Human hepatotoxicity	0.89	**P**	0.84	**P**	0.983	**P**	0.954	**P**	0.761	**P**
Drug-induced nephrotoxicity	0.991	**P**	0.97	**P**	0.984	**P**	1	**P**	0.986	**P**
Drug-induced neurotoxicity	0.996	**P**	0.992	**P**	0.98	**P**	1	**P**	0.965	**P**
Ototoxicity	0.389	**M**	0.178	**E**	0.009	**E**	0.869	**P**	0.45	**M**
Hematotoxicity	0.77	**P**	0.768	**P**	0.894	**P**	0.951	**P**	0.423	**M**
Genotoxicity	0.999	**P**	0.998	**P**	1	**P**	1	**P**	0.752	**P**
RPMI-8226 immunotoxicity	0.026	**E**	0.021	**E**	0.012	**E**	0.954	**P**	0.254	**E**
A549 cytotoxicity	0.087	**E**	0.035	**E**	0.016	**E**	1	**P**	0.369	**M**
Hek293 cytotoxicity	0.625	**M**	0.517	**M**	0.738	**P**	0.992	**P**	0.867	**P**
BCF	2.151		1.41		1.639		0.528		1.727	
IGC50	4.784		4.615		5.119		3.549		3.842	
LC50DM	6.246		5.846		6.443		5.09		5.126	
LC50FM	5.908		5.53		6.188		4.397		4.593	

[a] According to literature report, PTX – paclitaxel, GEF – Gefitinib, Caco-2 permeability (optimal: higher than −5.15 log unit), MDCK permeability (low permeability: $< 2 \times 10^{-6}$ cm s^{-1}, medium permeability: 2–20 $\times 10^{-6}$ cm s^{-1}, high passive permeability: $>20 \times 10^{-6}$ cm s^{-1}), PAMPA – the experimental data for P_{eff} was logarithmically transformed ($\log P_{eff} < 2$: low-permeability, $\log P_{eff} > 2.5$: high-permeability), Pgp – P-glycoprotein, HIA – Human Intestinal Absorption (−: ≥30%, +: <30%), *F*: bioavailability (+: <percent value, −: ≥percent value), PPB: Plasma Protein Binding (optimal: <90%), VD: Volume Distribution (optimal: 0.04–20 L kg^{-1}), BBB: Blood–Brain Barrier Penetration, Fu: The fraction unbound in plasms (low: <5%, middle: 5–20%, high: >20%), CL: clearance (low: <5 mL min^{-1} kg^{-1}, moderate: 5–15 mL min^{-1} kg^{-1}, high: >15 mL min^{-1} kg^{-1}), $T_{1/2}$ (ultra-short half-life drugs: 0.5 ≤ 1 h; short half-life drugs: 1–4 h; intermediate short half-life drugs: 4–8 h; long half-life drugs: >8 h), hERG blockers (IC_{50} ≤ 10 μM or ≥50% inhibition at 10 μM were classified as hERG +, IC_{50} > 10 μM or <50% inhibition at 10 μM were classified as hERG), DILI: Drug-Induced Liver Injury, Rat Oral Acute Toxicity (0: low-toxicity > 500 mg kg^{-1}, 1: high-toxicity < 500 mg kg^{-1}), FDAMDD – Maximum Recommended Daily Dose, BCF – Bioconcentration Factors, IGC50 – tetrahymena pyriformis 50 percent growth inhibition concentration, LC50FM – 96 h fathead minnow 50 percent lethal concentration, LC50DM – 48 h daphnia magna 50 percent lethal concentration. The output value is the probability of being inhibitor/substrate/active/positive/high-toxicity/sensitizer/carcinogens/corrosives/irritants (category 1) or non-inhibitor/non-substrate/inactive/negative/low-toxicity/non-sensitizer/non-carcinogens/noncorrosives/nonirritants (category 0). For the classification endpoints, the prediction probability values are transformed into six symbols: 0–0.1(−−−), 0.1–0.3(−−), 0.3–0.5(−), 0.5–0.7(+), 0.7–0.9(++), and 0.9–1.0(+++). Additionally, the corresponding relationships of the three labels are as follows: **E** – excellent, **M** – medium, **P** – poor.

In distribution, compounds **5**, **6**, and **7** showed poor to medium parameters such as PPB (%), Fu (%), OATP1B1 inhibitor, OATP1B3 inhibitor, BCRP inhibitor, and BSEP inhibitor. These showed good plasma protein binding capacity with PPB > 90% compared to PTX compounds (PPB = 93%). However, the optimal PPB needs to be less than 90%, like the GEF. In contrast, these compounds showed two excellent parameters, including VD (optimal: 0.04–20 L kg^{-1}) and MRP1 inhibitor. In addition, studying the BBB (Blood–Brain Barrier) permeability, compound **6** demonstrated no ability to penetrate the BBB, similar to reference drugs PTX and GEF.

In metabolism, compounds **5**, **6**, and **7** were predicted to be potent inhibitors of cytochrome enzymes CYP1A2, CYP2C19, CYP2C9, and CYP2C8. Additionally, compound **6** demonstrated strong inhibition of CYP3A4 as a main enzyme involved in drug metabolism, whereas compounds **5** and **7** did not exhibit inhibition of this enzyme.

In excretion, the CL (clearance) is a significant parameter in deciding dose intervals as a tool for the assessment of excretion. All active compounds and PTX showed lower CL values and were classified as low clearance levels (CL < 5 mL min^{-1} kg^{-1}) compared to GEF (moderate CL = 5–15 mL min^{-1} kg^{-1}). Therefore, compounds **5**, **6**, and **7** exhibited slower clearance rates, which means they require longer dosing intervals.

Finally, in toxicity, compounds **5**, **6**, and **7** showed poor parameters such as DILI (drug-induced liver injury), AMES toxicity, FDAMDD (maximum recommended daily dose), skin sensitization, carcinogenicity, eye irritation, human hepatotoxicity, drug-induced nephrotoxicity, drug-induced neurotoxicity, hematotoxicity, genotoxicity, and Hek293 cytotoxicity. However, these compounds did not show rat oral acute toxicity, eye corrosion, ototoxicity, RPMI-8226 immunotoxicity, and A549 cytotoxicity. Overall, the toxicity of the potential compounds was similar to that of the reference drugs PTX and GEF.

ADMETlab 3.0 and SwissADME are powerful computational tools designed to predict the absorption, distribution, metabolism, excretion, and toxicity (ADMET) properties of small molecules, offering significant advantages in drug discovery such as a robust database, advanced machine learning algorithms, and integration of diverse molecular descriptors. However, limitations exist, such as the potential for inaccuracies in predictions for compounds outside the training dataset's chemical space, as seen in cases such as the mispredicted P-gp substrate status of Gefitinib. The model's dependence on specific descriptors may also miss complex biological interactions, requiring experimental validation. These limitations highlight the need for careful interpretation and additional experimental studies to ensure accuracy.

2.4 *In silico* molecular docking study

Quinazolone derivatives have been shown to have anticancer mechanisms through the inhibition of multiple tyrosine kinases.[33,34] Therefore, the potential derivatives were evaluated for their ability to bind to EGFR using the molecular docking study (Table 4 and Fig. 4). Compounds **5**, **6**, and **7** showed strong interactions with the EGFR target with binding affinities of −9.6, −10.1, and −9.8 kcal mol^{-1}, respectively. In particular, these compounds were shown to have stronger binding affinities than the reference drug GEF at the EGFR active site. The aromatic groups of these compounds played a key role in binding to EGFR through multiple hydrophobic interactions.

In addition, compound **5** formed one halogen bond (3.05 Å, ASP855), one electrostatic π–cation interaction (4.35 Å, LYS745), and hydrophobic interactions (π–σ and π–alkyl) at amino acids LEU718, VAL726, LYS745, ALA743, and LEU844 (3.97–5.47 Å). Compound **7** established one strong hydrogen bond (2.25 Å, THR854) and hydrophobic interactions (π–σ and π–alkyl) at amino acids LEU718, VAL726, ALA743, and LYS745 (3.60–4.93 Å). Meanwhile, compound **6** only exhibited hydrophobic interactions (π–σ and π–alkyl) at amino acids LEU718, VAL726, LYS745, ALA743, and LEU844, with bond lengths ranging from 3.75 to 5.31 Å. Notably, three potential compounds exhibited

Table 4 *In silico* molecular docking results of active compounds and reference drug[a]

Ligand	Affinity binding (kcal mol^{-1})	Distance (Å)	Category	Types	Amino acid
5	**−9.6**	3.05	Halogen	Halogen (fluorine)	ASP855
		4.35	Electrostatic	π–cation	LYS745
		3.97	Hydrophobic	π–σ	LEU718
		4.83	Hydrophobic	π–alkyl	VAL726
		4.00	Hydrophobic	π–alkyl	LYS745
		5.47	Hydrophobic	π–alkyl	VAL726
		4.58	Hydrophobic	π–alkyl	ALA743
		4.98	Hydrophobic	π–alkyl	LEU844
6	**−10.1**	3.75	Hydrophobic	π–σ	LEU718
		4.85	Hydrophobic	π–alkyl	VAL726
		4.43	Hydrophobic	π–alkyl	LYS745
		5.08	Hydrophobic	π–alkyl	ALA743
		5.31	Hydrophobic	π–alkyl	LEU844
7	**−9.8**	2.25	Hydrogen bond	CHB	THR854
		3.60	Hydrophobic	π–σ	LEU718
		4.45	Hydrophobic	π–alkyl	VAL726
		4.79	Hydrophobic	π–alkyl	VAL726
		4.93	Hydrophobic	π–alkyl	ALA743
		4.48	Hydrophobic	π–alkyl	LYS745
GEF	**−7.8**	2.29	Hydrogen bond	CHB	MET793
		3.29	Hydrogen bond	CarHB	LEU718
		3.36	Hydrogen bond	CarHB	GLN791
		3.32	Hydrogen bond	CarHB	MET793
		2.91	Halogen	Halogen (fluorine)	GLU762
		3.31	Hydrophobic	π–σ	LEU844
		4.17	Hydrophobic	Alkyl	LEU718
		5.46	Hydrophobic	Alkyl	LEU792
		4.11	Hydrophobic	Alkyl	LYS745
		5.42	Hydrophobic	Alkyl	MET766
		4.33	Hydrophobic	Alkyl	LEU788
		4.75	Hydrophobic	π–alkyl	LEU718
		5.24	Hydrophobic	π–alkyl	VAL726
		4.58	Hydrophobic	π–alkyl	ALA743
		4.97	Hydrophobic	π–alkyl	LEU844
		3.50	Hydrophobic	π–alkyl	ALA743
		4.15	Hydrophobic	π–alkyl	LYS745

[a] CHB – conventional hydrogen bond (strong hydrogen bond), CarHB – carbon–hydrogen bond, GEF – Gefitinib.

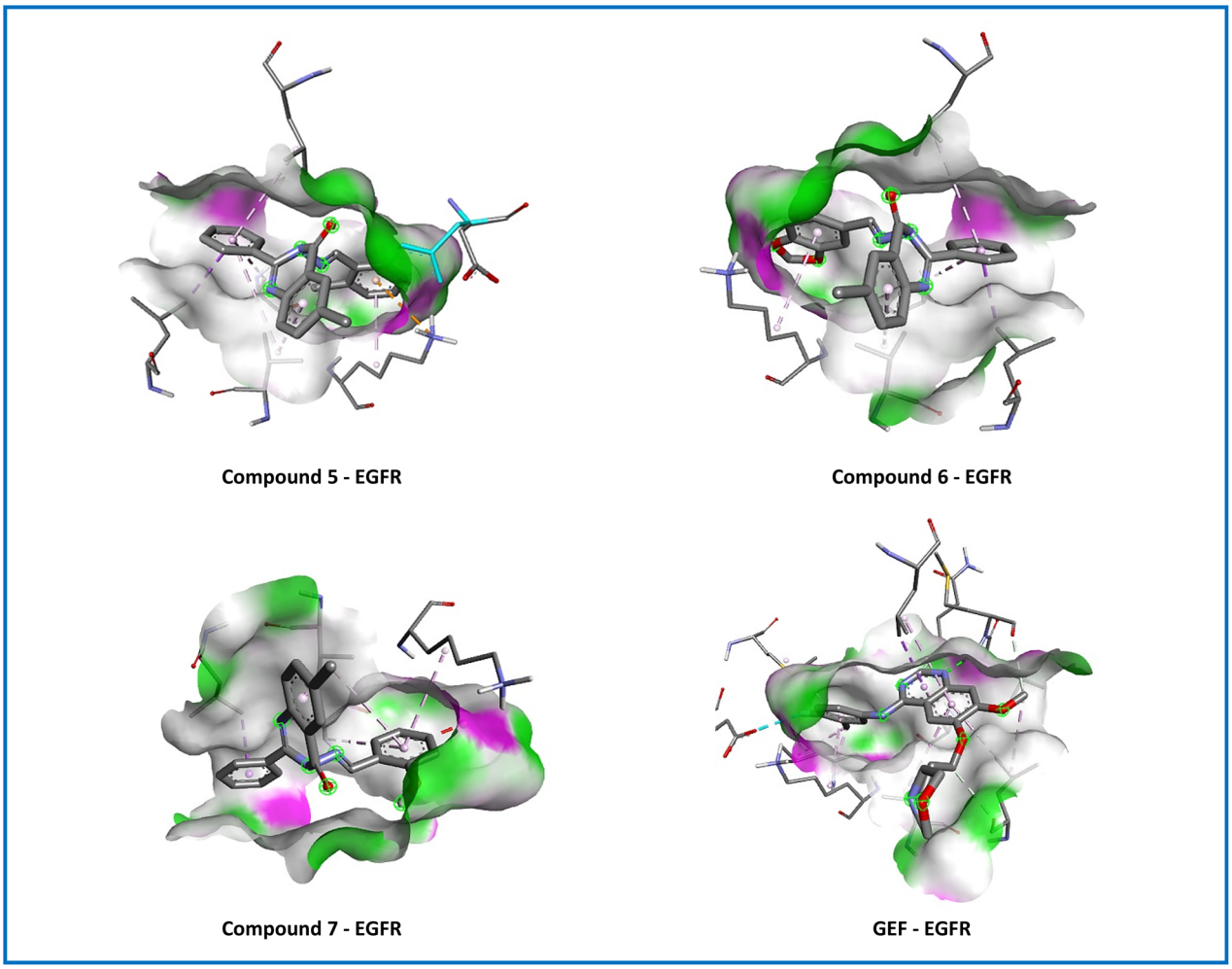

Fig. 4 3D representation of the interaction of potential compounds **5–7** and Gefitinib (GEF) with epidermal growth factor receptor (EGFR) (*Spodoptera frugiperda*).

interactions with amino acids LYS745, LEU718, VAL726, ALA743, and LEU844, similar to the co-crystallized ligand and reference drug GEF. Therefore, molecular docking results showed that strong EGFR inhibition may be responsible for the potent and selective anticancer activity of these compounds. However, these findings need to be confirmed by *in vitro* binding studies of compounds **5**, **6**, and **7** to the EGFR target. Furthermore, to elucidate the mechanisms underlying the observed cytotoxicity of these compounds, further investigation into alternative molecular targets or potential off-target effects is necessary.

3. Experimental section

3.1 Materials

Benzoyl chloride, 5-chloroanthranilic acid, and hydrazine hydrate were purchased from Acros (Belgium). Benzaldehyde derivatives, other catalysts, reagents, solvents, and chemicals were obtained from Merck (Germany). Thin-layer chromatography (TLC) on silica gel plates coated with fluorescent indicator F_{254} (Merck) was employed to monitor the completion of reactions.

The melting points of all products were recorded using the Sanyo Gallenkamp melting point apparatus. Infrared spectra were obtained on the IRAffinity-1S FT-IR spectrophotometer from Shimadzu. Synthesized substances underwent molecular characterization through mass spectrometry on an Agilent LC-MS instrument and nuclear magnetic resonance (NMR) spectroscopy recorded on Bruker Avance III 500 MHz. DMSO-d_6 was utilized as a solvent for all compounds. Coupling constants (J) and chemical shifts (δ) were given in Hz and ppm, respectively.

3.2 Experimental procedures

3.2.1 Procedure for the preparation of 6-chloro-2-phenyl-4*H*-benzo[*d*][1,3]oxazin-4-one (Q0). In a double-neck flask, a mixture of 5-chloroanthranilic acid (0.1 mol) and pyridine (dried, 120 mL) is dissolved and refluxed for 10–15 minutes. The mixture is then cooled to 0–5 °C for 30 minutes. Benzoyl chloride (3.2 mL) is added dropwise (1 drop per second) to the mixture, followed by continuously stirring for 2 hours. The mixture is kept cool at 0–5 °C throughout the process.

Once the reaction completion is confirmed on TLC, the reaction mixture is left at room temperature. The aqueous

solution of saturated Na_2CO_3 (100 mL) is added gradually (10 mL each time) until the pH of the mixture reaches 7. When the product crystallizes, it is filtered, washed with cold water, and dried under a vacuum to yield **Q0**. Synthesis yield: 85%.

*3.2.1.1 6-Chloro-2-phenyl-4H-benzo[d][1,3]oxazin-4-one (**Q0**).* Green powder, mp 194–195 °C. ^{1}H NMR (500 MHz, DMSO-d_6, δ ppm): 8.20 (2H, d, J = 7.0 Hz, H–Ar), 8.13 (1H, s, H–Ar), 7.98 (1H, d, J = 7.5 Hz, H–Ar), 7.75 (1H, d, J = 8.0 Hz, H–Ar), 7.69–7.67 (1H, m, H–Ar), 7.63–7.61 (2H, m, H–Ar). ^{13}C NMR (125 MHz, DMSO-d_6, δ ppm): 157.9; 156.7; 145.1; 136.6; 132.9; 132.4; 129.8; 129.0; 129.0; 127.9; 127.0; 118.6. LC-MS (m/z) $[M + H]^+$ calcd for $C_{14}H_9ClNO_2$ 258.0316, found 258.0344.

3.2.2 Procedure for the preparation of 3-amino-6-chloro-2-phenyl-4(3*H*)-quinazolone (1). A mixture of pyridine (20 mL) and **Q0** (0.05 mol) is stirred for 10 minutes and refluxed at 10 °C until completely dissolves. Hydrazine hydrate (0.03 mol) is added gradually to the reaction mixture. The reaction mixture is stirred and refluxed for 2 hours until the **Q0** sample disappears on the TLC plate.

Concentrated sulfuric acid and polyphosphoric acid (PPA) are subsequently added and the reaction mixture is refluxed for 2 hours. The product precipitates as white crystals. When TLC shows the completion of the reaction, the reaction mixture is then left at room temperature and cooled to 0–5 °C. An aqueous solution of 10% NaOH (25 mL) is added dropwise to neutralize the mixture to pH 8 and therefore, more crystals can be observed.

The obtained mixture is filtered, washed with cold water and dried under vacuum to yield **1**. Synthesis yield: 66%.

*3.2.2.1 3-Amino-6-chloro-2-phenyl-4(3H)-quinazolinone (**1**).* White to beige crystal, mp 169–172 °C. ^{1}H NMR (500 MHz, DMSO-d_6, δ ppm): 8.09 (1H, s, H–Ar), 7.82–7.81 (3H, m, H–Ar), 7.72 (1H, d, J = 3.5 Hz, H–Ar), 7.49–7.48 (3H, m, H–Ar), 5.70 (2H, s, NH_2). ^{13}C NMR (125 MHz, DMSO-d_6, δ ppm): 160.3, 156.2, 145.4, 134.5, 134.4, 130.9, 129.7, 129.6, 129.6, 127.4, 124.9, 121.2. LC-MS (m/z) $[M–H]^-$ calcd for $C_{14}H_9ClN_3O$ 270.0440, found 270.0437.

3.2.3 General procedure for the preparation of *N*-imine derivatives of 6-chloro-2-(phenyl-4(3*H*)-quinazolinone-3-yl)-*N*-aryl imine (2–21). In a double-neck flask, compound **1** (0.1 mol) is dissolved and refluxed at 80 °C in ethanol absolute (30 mL). Aldehyde derivative (0.1 mol) is added and the mixture is refluxed for 1–2 hours. Once the reaction has finished, the mixture is cooled to 0–5 °C, and the product is filtered and washed with cold water. Recrystallization with the ethanol–water mixture is conducted to obtain pure products. The crystals of compounds **2–21** are dried at 60 °C under vacuum. Synthesis yield: 68–90%.

*3.2.3.1 6-Chloro-3-((4-nitrobenzylidene)amino)-2-phenyl-4(3H)-quinazolone (**2**).* White solid, mp 238–241 °C. ^{1}H NMR (500 MHz, DMSO-d_6, δ ppm): 9.30 (1H, s, –CH═N), 8.34 (2H, d, J = 8.5 Hz, H–Ar), 8.19 (1H, d, J = 2.0 Hz, H–Ar), 7.99–7.94 (3H, m, H–Ar), 7.84 (1H, d, J = 9.0 Hz, H–Ar), 7.72 (2H, d, J = 7.5 Hz, H–Ar), 7.51–7.45 (3H, m, H–Ar). ^{13}C NMR (125 MHz, DMSO-d_6, δ ppm): 166.0, 156.6, 153.2, 149.4, 144.6, 137.7, 134.5, 134.0, 131.2, 129.6, 129.5, 129.3, 129.2, 127.3, 125.3, 123.7, 122.1. LC-MS (m/z) $[M + H]^+$ calcd for $C_{21}H_{14}ClN_4O_3$ 405.0749, found 405.0792.

*3.2.3.2 6-Chloro-3-((3,4-dichlorobenzylidene)amino)-2-phenyl-4(3H)-quinazolone (**3**).* White solid, mp 225–226 °C. ^{1}H NMR (500 MHz, DMSO-d_6, δ ppm): 9.13 (1H, s, –CH═N), 8.17 (1H, d, J = 2.0 Hz, H–Ar), 7.93–7.94 (2H, m, H–Ar), 7.82 (1H, d, J = 8.5 Hz, H–Ar), 7.78 (1H, d, J = 8.5 Hz, H–Ar), 7.70–7.68 (3H, m, H–Ar), 7.52–7.45 (3H, m, H–Ar). ^{13}C NMR (125 MHz, DMSO-d_6, δ ppm): 165.8, 156.7, 144.7, 134.9, 134.6, 134.0, 132.7, 131.9, 131.3, 131.2, 129.7, 129.6, 129.4, 127.9, 127.4, 125.4, 122.1. LC-MS (m/z) $[M + H]^+$ calcd for $C_{21}H_{13}Cl_3N_3O$ 428.0119, found 428.0130.

*3.2.3.3 6-Chloro-3-((4-fluorobenzylidene)amino)-2-phenyl-4(3H)-quinazolone (**4**).* White solid, mp 207–208 °C. ^{1}H NMR (500 MHz, DMSO-d_6, δ ppm): 9.04 (1H, s, –CH═N), 8.17 (1H, d, J = 2.5 Hz, H–Ar), 7.93 (1H, dd, J = 8.5, 2.5 Hz, H–Ar), 7.83–7.78 (3H, m, H–Ar), 7.69 (2H, d, J = 7.0 Hz, H–Ar), 7.50–7.43 (3H, m, H–Ar), 7.37–7.34 (2H, m, H–Ar). ^{13}C NMR (125 MHz, DMSO-d_6, δ ppm): 168.5, 156.9, 153.5, 145.1, 134.8, 134.2, 131.4, 131.2, 131.1, 130.0, 129.9, 129.7, 128.8, 127.7, 125.6, 122.3, 116.4, and 116.2 ($J_{C–F}$ = 25.0 Hz). LC-MS (m/z) $[M + H]^+$ calcd for $C_{21}H_{14}ClFN_3O$ 378.0804, found 378.0814.

*3.2.3.4 6-Chloro-3-((2-chloro-6-fluorobenzylidene)amino)-2-phenyl-4(3H)-quinazolone (**5**).* White solid, mp 205–208 °C. ^{1}H NMR (500 MHz, DMSO-d_6, δ ppm): 9.31 (1H, s, –CH═N), 8.20 (1H, d, J = 2.0 Hz, H–Ar), 7.93 (1H, dd, J = 8.5, 2.5 Hz, H–Ar), 7.81 (1H, d, J = 8.5 Hz, H–Ar), 7.69 (2H, d, J = 7.5 Hz, H–Ar), 7.63–7.59 (1H, m, H–Ar), 7.49–7.37 (4H, m, H–Ar), 7.35 (1H, dd, J = 9.5, 9.5 Hz, H–Ar). ^{13}C NMR (125 MHz, DMSO-d_6, δ ppm): 164.2, 156.7, 153.4, 145.0, 135.0, 134.8, 134.3, 134.2, 131.4, 129.9, 129.8, 129.7, 127.6, 126.6, 125.8, 122.5, 118.7, 116.0, 115.9, and 115.8 ($J_{C–F}$ = 12.5 Hz). LC-MS (m/z) $[M + H]^+$ calcd for $C_{21}H_{13}Cl_2FN_3O$ 412.0414, found 412.0441.

*3.2.3.5 3-((Benzo[d][1,3]dioxol-5-ylmethylene)amino)-6-chloro-2-phenyl-4(3H)-quinazolone (**6**).* White solid, mp 215–217 °C. ^{1}H NMR (500 MHz, DMSO-d_6, δ ppm): 8.86 (1H, s, –CH═N), 8.16 (1H, d, J = 2.5 Hz, H–Ar), 7.92 (1H, dd, J = 8.5, 2.5 Hz, H–Ar), 7.80 (1H, d, J = 8.5 Hz, H–Ar), 7.69–7.68 (2H, m, H–Ar), 7.48–7.43 (3H, m, H–Ar), 7.27 (1H, dd, J = 8.0, 2.5 Hz, H–Ar), 7.18 (1H, d, J = 1.0 Hz, H–Ar), 7.05 (1H, d, J = 8.0 Hz, H–Ar), 6.12 (2H, s, –OCH_2O–). ^{13}C NMR (125 MHz, DMSO-d_6, δ ppm): 169.0, 156.9, 153.5, 151.4, 148.1, 145.1, 134.7, 134.3, 131.3, 129.9, 129.8, 129.7, 127.7, 126.6, 126.4, 125.5, 122.3, 108.6, 105.5, 102.0. LC-MS (m/z) $[M + H]^+$ calcd for $C_{22}H_{15}ClN_3O_3$ 404.0797, found 404.0742.

3.2.3.6 3-((4-Bromo-2-hydroxybenzylidene)amino)-6-chloro-2-phenyl-4(3H)-quinazolone (7). White to light yellow solid, mp 247–248 °C. ^{1}H NMR (500 MHz, DMSO-d_6, δ ppm): 9.21 (1H, s, –CH═N), 8.17 (1H, d, J = 2.5 Hz, H–Ar), 7.92 (1H, dd, J = 8.5, 2.5 Hz, H–Ar), 7.81 (1H, d, J = 9.0 Hz, H–Ar), 7.68 (2H, d, J = 7.0 Hz, H–Ar), 7.60–7.58 (1H, m, H–Ar), 7.54 (1H, dd, J = 9.0, 2.5 Hz, H–Ar), 7.51–7.45 (3H, m, H–Ar), 6.92 (1H, d, J = 9.0 Hz, H–Ar). ^{13}C NMR (125 MHz, DMSO-d_6, δ ppm): 164.4, 157.9, 157.0, 153.6, 145.0, 136.4, 134.7, 134.4, 131.3, 129.9, 129.8, 129.6, 129.2, 127.7, 125.6, 122.5, 120.4, 119.1, 110.5. LC-MS (m/z) $[M + H]^+$ calcd for $C_{21}H_{14}BrClN_3O_2$ 453.9952, found 453.9970; $[M–H]^-$ calcd for $C_{21}H_{12}BrClN_3O_2$ 451.9807, found 451.9809.

*3.2.3.7 6-Chloro-3-((4-(dimethylamino)benzylidene)amino)-2-phenyl-4(3H)-quinazolone (**8**).* White solid, mp 220–221 °C. ^{1}H NMR (500 MHz, DMSO-d$_6$, δ ppm): 8.65 (1H, s, –CH=N), 8.15 (1H, d, J = 2.5 Hz, H–Ar), 7.90 (1H, dd, J = 8.5, 2.5 Hz, H–Ar), 7.80 (1H, d, J = 8.5 Hz, H–Ar), 7.68 (2H, d, J = 7.0 Hz, H–Ar), 7.53 (2H, d, J = 9.0 Hz, H–Ar), 7.47–7.41 (3H, m, H–Ar), 6.74 (2H, d, J = 8.5 Hz, H–Ar), 3.01 (6H, s, –N(CH$_3$)$_2$). ^{13}C NMR (125 MHz, DMSO-d$_6$, δ ppm): 169.8, 157.2, 153.7, 153.1, 145.2, 134.4, 131.1, 130.4, 129.7, 127.4, 125.4, 122.4, 118.8, 111.5. LC-MS (m/z) [M + H]$^+$ calcd for $C_{23}H_{20}ClN_4O$ 403.1320, found 403.1334.

*3.2.3.8 6-Chloro-3-((3-hydroxybenzylidene)amino)-2-phenyl-4(3H)-quinazolone (**9**).* White to beige solid, mp 255–257 °C. ^{1}H NMR (500 MHz, DMSO-d$_6$, δ ppm): 9.78 (1H, s, –OH), 8.92 (1H, s, –CH=N), 8.17 (1H, s, H–Ar), 7.92 (1H, d, J = 8.5 Hz, H–Ar), 7.81 (1H, d, J = 9.0 Hz, H–Ar), 7.68 (2H, d, J = 7.5 Hz, H–Ar), 7.49–7.44 (3H, m, H–Ar), 7.39–7.32 (1H, m, H–Ar), 7.15–7.12 (2H, m, H–Ar), 6.97 (1H, d, J = 8.5 Hz, H–Ar). ^{13}C NMR (125 MHz, DMSO-d$_6$, δ ppm): 170.2, 157.7, 153.4, 145.1, 134.7, 134.2, 133.3, 131.3, 130.2, 130.0, 129.8, 129.7, 127.7, 125.6, 120.4, 120.0, 113.9. LC-MS (m/z) [M + H]$^+$ calcd for $C_{21}H_{15}ClN_3O_2$ 376.0847, found 376.0839.

*3.2.3.9 6-Chloro-3-((4-ethoxy-3-hydroxybenzylidene)amino)-2-phenyl-4(3H)-quinazolone (**10**).* White to beige solid, mp 210–212 °C. ^{1}H NMR (500 MHz, DMSO-d$_6$, δ ppm): 8.78 (1H, s, –CH=N), 8.15 (1H, d, J = 2.0 Hz, H–Ar), 7.91 (1H, dd, J = 9.0, 2.5 Hz, H–Ar), 7.80 (1H, d, J = 8.5 Hz, H–Ar), 7.70 (2H, d, J = 7.5 Hz, H–Ar), 7.47–7.43 (3H, m, H–Ar), 7.20 (1H, s, H–Ar), 7.17 (1H, d, J = 8.0 Hz, H–Ar), 6.88 (1H, d, J = 8.0 Hz, H–Ar), 3.97 (2H, q, J = 7.0 Hz, –CH$_2$–), 1.31 (3H, t, J = 7.0 Hz, –CH$_3$). ^{13}C NMR (125 MHz, DMSO-d$_6$, δ ppm): 169.2, 157.0, 153.6, 151.7, 147.1, 145.1, 134.6, 134.3, 131.2, 129.8, 129.8, 127.6, 125.5, 124.3, 123.4, 122.4, 115.6, 111.6, 63.8, 14.5. LC-MS (m/z) [M + H]$^+$ calcd for $C_{23}H_{19}ClN_3O_3$ 420.1109, found 420.1125.

*3.2.3.10 6-Chloro-3-((2,4-dichlorobenzylidene)amino)-2-phenyl-4(3H)-quinazolone (**11**).* White to beige solid, mp 198–200 °C. ^{1}H NMR (500 MHz, DMSO-d$_6$, δ ppm): 9.45 (1H, s, –CH=N), 8.19 (1H, d, J = 2.0 Hz, H–Ar), 7.93 (1H, dd, J = 9.0, 2.5 Hz, H–Ar), 7.84–7.80 (2H, m, H–Ar), 7.69 (2H, d, J = 7.0 Hz, H–Ar), 7.66 (1H, d, J = 8.5 Hz, H–Ar), 7.53–7.45 (4H, m, H–Ar). ^{13}C NMR (125 MHz, DMSO-d$_6$, δ ppm): 163.1, 156.8, 153.3, 144.6, 137.6, 135.5, 134.4, 134.1, 131.2, 129.6, 129.5, 129.4, 129.3, 128.7, 128.6, 127.9, 127.3, 125.4, 122.2. LC-MS (m/z) [M + H]$^+$ calcd for $C_{21}H_{13}Cl_3N_3O$ 428.0119, found 428.0141.

*4.2.3.11 6-Chloro-3-((2-chlorobenzylidene)amino)-2-phenyl-4(3H)-quinazolinone (**12**).* White to beige solid, mp 223–224 °C. ^{1}H NMR (500 MHz, DMSO-d$_6$, δ ppm): 9.46 (1H, s, –CH=N), 8.21 (1H, d, J = 2.5 Hz, H–Ar), 7.93 (1H, dd, J = 2.5, 8.5 Hz, H–Ar), 7.82 (1H, d, J = 8.5 Hz, H–Ar), 7.68–7.71 (3H, m, H–Ar), 7.58–7.64 (2H, m, H–Ar), 7.46–7.52 (3H, m, H–Ar), 7.43–7.40 (1H, m, H–Ar). ^{13}C NMR (125 MHz, DMSO-d$_6$, δ ppm): 164.6, 164.4, 156.7, 153.3, 148.4, 144.7, 134.7, 134.4, 134.1, 133.5, 131.1, 129.9, 129.7, 129.5, 129.4, 129.3, 127.5, 127.4, 127.3, 125.4, 122.2, 119.2. LC-MS (m/z) [M + H]$^+$ calcd for $C_{21}H_{14}Cl_2N_3O$ 394.0509, found 394.0513.

*3.2.3.12 6-Chloro-3-((3,4-dimethoxybenzylidene)amino)-2-phenyl-4(3H)-quinazolone (**13**).* White to beige powder, mp 176–177 °C. ^{1}H NMR (500 MHz, DMSO-d$_6$, δ ppm): 8.88 (1H, s, –CH=N), 8.16 (1H, d, J = 2.0 Hz, H–Ar), 7.91 (1H, dd, J = 9.0, 2.5 Hz, H–Ar), 7.81 (1H, d, J = 9.0 Hz, H–Ar), 7.71 (2H, d, J = 7.0 Hz, H–Ar), 7.49–7.43 (3H, m, H–Ar), 7.30 (1H, d, J = 8.0 Hz, H–Ar), 7.24 (1H, s, H–Ar), 7.07 (1H, d, J = 8.0 Hz, H–Ar), 3.83 (3H, s, –OCH$_3$), 3.71 (3H, s, –OCH$_3$). ^{13}C NMR (125 MHz, DMSO-d$_6$, δ ppm): 168.2, 156.9, 153.5, 152.8, 149.0, 144.9, 134.3, 134.2, 131.1, 129.5, 129.5, 129.5, 127.3, 125.2, 124.8, 123.8, 122.2, 111.7, 109.9; 55.60, 55.40. LC-MS (m/z) [M–H]$^-$ calcd for $C_{23}H_{17}ClN_3O_3$ 418.0964, found 418.0973.

*3.2.3.13 6-Chloro-2-phenyl-3-((pyridin-3-ylmethylene)amino)-4(3H)-quinazolone (**14**).* White to beige solid, mp 184–186 °C. ^{1}H NMR (500 MHz, DMSO-d$_6$, δ ppm): 9.18 (1H, s, H–Ar), 8.87 (1H, s, –CH=N), 8.75–8.74 (1H, dd, J = 4.5, 1.0 Hz, H–Ar), 8.18 (1H, d, J = 2.0, H–Ar), 8.07 (1H, d, J = 8.0 Hz, H–Ar), 7.93 (1H, dd, J = 8.5, 2.0 Hz, H–Ar), 7.82 (1H, d, J = 8.5 Hz, H–Ar), 7.71 (2H, d, J = 7.0, H–Ar), 7.55–7.44 (4H, m, H–Ar). ^{13}C NMR (125 MHz, DMSO-d$_6$, δ ppm): 166.9, 156.9, 153.5, 153.1, 149.9, 145.0, 134.9, 134.9, 134.2, 131.4, 130.0, 129.9, 129.7, 128.2, 127.7, 125.6, 124.3, 122.3. LC-MS (m/z) [M + H]$^+$ calcd for $C_{20}H_{14}ClN_4O$ 361.0851, found 361.0860.

*3.2.3.14 6-Chloro-3-((furan-2-ylmethylene)amino)-2-phenyl-4(3H)-quinazolone (**15**).* White to beige solid, mp 214–216 °C. ^{1}H NMR (500 MHz, DMSO-d$_6$, δ ppm): 8.85 (1H, s, –CH=N), 8.16 (1H, d, J = 2.5 Hz, H–Ar), 7.99 (1H, s, H–Ar), 7.92 (1H, dd, J = 9.0, 2.5 Hz, H–Ar), 7.80 (1H, d, J = 9.0 Hz, H–Ar), 7.67 (2H, d, J = 7.0 Hz, H–Ar), 7.50–7.44 (3H, m, H–Ar), 7.25 (1H, d, J = 3.5 Hz, H–Ar), 6.75–6.74 (1H, m, H–Ar). ^{13}C NMR (125 MHz, DMSO-d$_6$, δ ppm): 157.7, 156.7, 148.4, 147.7, 147.2, 146.4, 134.4, 134.2, 129.8, 129.6, 129.5, 129.4, 128.3, 127.7, 127.4, 125.3, 125.1, 122.1, 119.4, 112.5, 112.4. LC-MS (m/z) [M + H]$^+$ calcd for $C_{19}H_{13}ClN_3O_2$ 350.0691, found 350.1725.

*3.2.3.15 6-Chloro-3-((3-nitrobenzylidene)amino)-2-phenyl-4(3H)-quinazolone (**16**).* White solid, mp 227–229 °C. ^{1}H NMR (500 MHz, DMSO-d$_6$, δ ppm): 9.31 (1H, s, –CH=N), 8.49 (1H, s, H–Ar), 8.40 (1H, d, J = 8.5 Hz, H–Ar), 8.18 (1H, d, J = 2.5 Hz, H–Ar), 8.15 (1H, d, J = 7.5 Hz, H–Ar), 7.94 (1H, dd, J = 8.5, 2.5 Hz, H–Ar), 7.84–7.79 (2H, m, H–Ar), 7.71 (2H, d, J = 7.0 Hz, H–Ar), 7.52–7.45 (3H, m, H–Ar). ^{13}C NMR (125 MHz, DMSO-d$_6$, δ ppm): 166.1, 156.8, 153.4, 148.1, 144.7, 134.6, 134.1, 133.8, 131.3, 130.6, 129.7, 129.6, 129.4, 127.5, 126.4, 125.4, 122.4, 122.1. LC-MS (m/z) [M + H]$^+$ calcd for $C_{21}H_{14}ClN_4O_3$ 405.0749, found 405.0758.

*3.2.3.16 6-Chloro-3-((4-ethoxybenzylidene)amino)-2-phenyl-4(3H)-quinazolone (**17**).* White solid, mp 218–219 °C. ^{1}H NMR (500 MHz, DMSO-d$_6$, δ ppm): 8.87 (1H, s, –CH=N), 8.16 (1H, s, H–Ar), 7.91 (1H, dd, J = 8.5, 1.5 Hz, H–Ar), 7.81 (1H, d, J = 8.5 Hz, H–Ar), 7.69–7.65 (4H, m, H–Ar), 7.47–7.42 (3H, m, H–Ar), 7.03 (2H, d, J = 8.5 Hz, H–Ar), 4.11 (2H, q, J = 7.0 Hz, H–Ar), 1.34 (3H, t, J = 7.0 Hz, H–Ar). ^{13}C NMR (125 MHz, DMSO-d$_6$, δ ppm): 169.7, 169.6, 162.2, 159.6, 157.0, 145.1, 138.8, 134.7, 134.3, 131.3, 130.6, 129.8, 129.7, 127.7, 125.5, 124.4, 122.4, 115.0, 63.6, 14.5. LC-MS (m/z) [M + H]$^+$ calcd for $C_{23}H_{19}ClN_3O_2$ 404.1160, found 404.1186.

*3.2.3.17 6-Chloro-3-((3-methoxybenzylidene)amino)-2-phenyl-4(3H)-quinazolone (**18**).* White solid, mp 178–179 °C. ^{1}H NMR (500 MHz, DMSO-d$_6$, δ ppm): 9.02 (1H, s, –CH=N), 8.17 (1H, d, J

= 2.5 Hz, H–Ar), 7.93 (1H, dd, J = 9.0, 2.5 Hz, H–Ar), 7.82 (1H, d, J = 9.0 Hz, H–Ar), 7.70 (2H, d, J = 6.5 Hz, H–Ar), 7.50–7.41 (4H, m, H–Ar), 7.30 (1H, d, J = 8.5 Hz, H–Ar), 7.23 (1H, s, H–Ar), 7.17–7.15 (1H, m, H–Ar), 3.75 (3H, s, –OCH_3). ^{13}C NMR (125 MHz, DMSO-d_6, δ ppm): 169.1, 159.5, 156.9, 153.6, 145.0, 134.8, 134.3, 133.6, 131.4, 130.3, 129.9, 129.9, 129.7, 127.7, 125.6, 122.4, 121.5, 118.8, 112.6, 55.2. LC-MS (m/z) $[M + H]^+$ calcd for $C_{22}H_{17}ClN_3O_2$ 390.1004, found 390.1016.

*3.2.3.18 6-Chloro-3-((2-hydroxybenzylidene)amino)-2-phenyl-4(3H)-quinazolone (**19**).* White to beige solid, mp 211–213 °C. ^{1}H NMR (500 MHz, DMSO-d_6, δ ppm): 10.38 (1H, s, –OH), 9.18 (1H, s, –CH=N), 8.17 (1H, d, J = 2.5 Hz, H–Ar), 7.92 (1H, dd, J = 8.5, 2.0 Hz, H–Ar), 7.81 (1H, d, J = 8.5 Hz, H–Ar), 7.69 (2H, d, J = 7.0 Hz, H–Ar), 7.55 (1H, d, J = 7.0 Hz, H–Ar), 7.49–7.38 (4H, m, H–Ar), 6.94 (1H, d, J = 2.0 Hz, H–Ar), 6.89–6.86 (1H, m, H–Ar). ^{13}C NMR (125 MHz, DMSO-d_6, δ ppm): 167.2, 158.6, 157.0, 153.6, 145.1, 134.7, 134.4, 131.3, 129.9, 129.8, 129.6, 129.1, 128.2, 127.8, 125.6, 122.5, 119.6, 118.0, 116.7. LC-MS (m/z) $[M + H]^+$ calcd for $C_{21}H_{15}ClN_3O_2$ 376.0847, found 376.0839; $[M–H]^-$ calcd for $C_{21}H_{13}ClN_3O_2$ 374.0702, found 374.0696.

*3.2.3.19 6-Chloro-3-((3-hydroxy-4-methoxybenzylidene) amino)-2-phenyl-4(3H)-quinazolone (**20**).* White to beige solid, mp 240–242 °C. ^{1}H NMR (500 MHz, DMSO-d_6, δ ppm): 9.43 (1H, s, –OH), 8.77 (1H, s, –CH=N), 8.15 (1H, d, J = 2.5 Hz, H–Ar), 7.91 (1H, dd, J = 8.5, 2.0 Hz, H–Ar), 7.81 (1H, d, J = 8.5 Hz, H–Ar), 7.67 (2H, d, J = 6.5 Hz, H–Ar), 7.47–7.43 (3H, m, H–Ar), 7.16 (2H, d, J = 8.0 Hz, H–Ar), 7.03 (1H, d, J = 8.0 Hz, H–Ar), 3.83 (3H, s, –OCH_3). ^{13}C NMR (125 MHz, DMSO-d_6, δ ppm): 170.0, 156.9, 153.5, 152.0, 146.9, 145.1, 134.6, 134.3, 131.2, 129.9, 129.8, 129.7, 127.6, 125.5, 124.7, 123.0, 122.3, 113.1, 111.8, 55.7. LC-MS (m/z) $[M + H]^+$ calcd for $C_{22}H_{17}ClN_3O_3$ 406.0953, found 406.0964; $[M–H]^-$ calcd for $C_{22}H_{15}ClN_3O_3$ 404.0807, found 404.0798.

*3.2.3.20 3-(Benzylideneamino)-6-chloro-2-phenyl-4(3H)-quinazolone (**21**).* White needle-shaped crystal, mp 184–185 °C. ^{1}H NMR (500 MHz, DMSO-d_6, δ ppm): 9.03 (1H, s, –CH=N), 8.17 (1H, d, J = 2.5 Hz, H–Ar), 7.93 (1H, dd, J = 9.0, 2.5 Hz, H–Ar), 7.82 (1H, d, J = 9.0 Hz, H–Ar), 7.73–7.69 (4H, m, H–Ar), 7.61–7.58 (1H, m, H–Ar), 7.52–7.43 (5H, m, H–Ar). ^{13}C NMR (125 MHz, DMSO-d_6, δ ppm): 169.8, 156.9, 153.5, 145.0, 134.7, 134.2, 132.7, 132.1, 131.3, 129.9, 129.8, 129.7, 129.1, 128.6, 127.7, 125.6, 122.3. LC-MS (m/z) $[M + H]^+$ calcd for $C_{21}H_{15}ClN_3O$ 360.0898, found 360.0899.

3.3 *In vitro* cytotoxic activity

The cytotoxic activity of the quinazolinone derivatives was evaluated against two cancer cell lines (RD and MDA-MB-231) and one normal cell line (LLC-PK1) using the methylthiazolyl tetrazolium (MTT) method, conducted according to the MTT assay protocol. PTX was used as the positive control. The assay detects the reduction of yellow tetrazolium by metabolically active cells to purple formazan, which is measured using spectrophotometry. The cell lines were seeded into 96-well plates at a density of 5000 cells per well and incubated at 37 °C in 5% CO_2 for 24 h with growth media consisting of 2 mM L-glutamine, 100 IU mL^{-1} penicillin, 100 μg mL^{-1} streptomycin, Eagle's minimum essential medium, and 10% fetal calf serum. After that, a series of concentrations of the tested compounds and the reference drug PTX in DMSO was added to each well of the plate and incubated for 72 h. The 10 μL fresh solution of MTT reagent was added to each well, and the plate was incubated in a CO_2 incubator at 37 °C for 4 h until a purple precipitate appeared. Finally, the cells were solubilized in ethanol, and their optical density was recorded at 570 nm.[35,36] The percent of proliferation inhibition was calculated using the following formula:

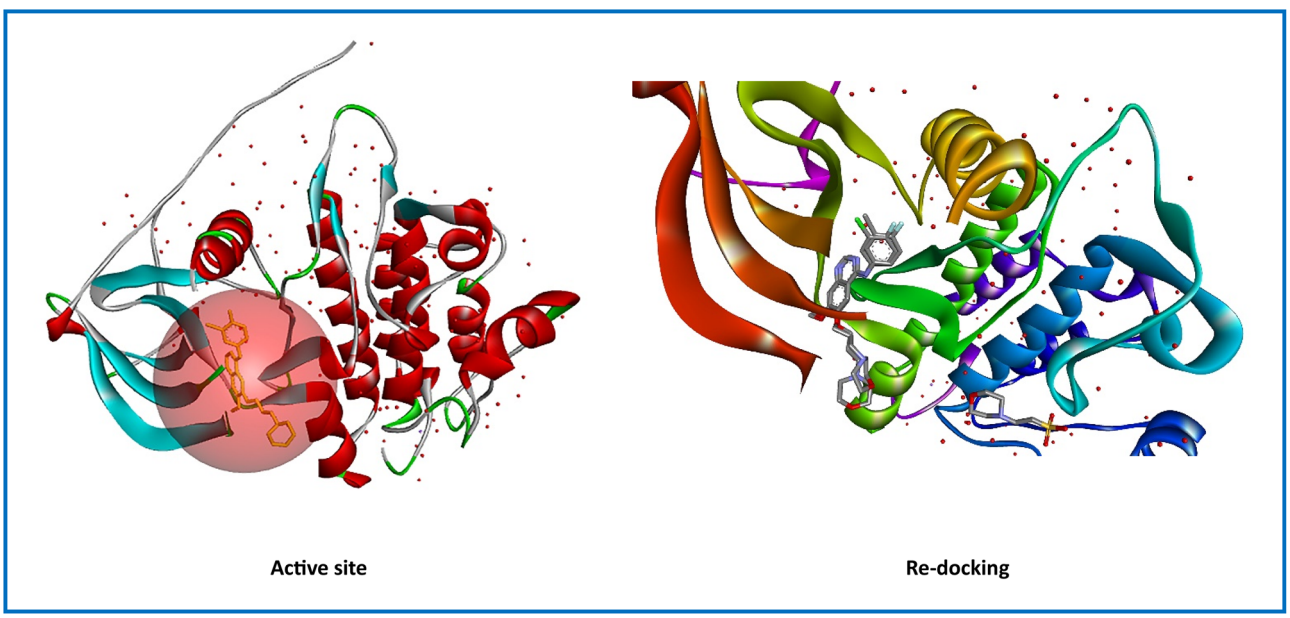

Fig. 5 Active site and re-docking result of EGFR target.

$$\text{Viability cells inhibition } (\%) = 100 - \left[\frac{(A_t - A_b)}{(A_c - A_b)}\right] \times 100\%$$

A_t = absorption of test compound, A_b = absorption of blank, A_c = absorption of control.

3.4 ADME-Tox predictions

The physicochemical properties were calculated using the SwissADME tool. The *in silico* ADMET properties were performed using ADMETlab 3.0 descriptors algorithm protocol.[37]

3.5 *In silico* molecular docking study

The energy of ligands was minimized using ChemBio3D Ultra 19.0. Ligands were then used as input for AutoDock Vina in order to carry out the docking simulation. The EGFR anticancer target (ID PDB: 4WKQ) was retrieved from the protein data bank. EGFR was removed water molecules and added only polar hydrogen and Kollman charges. The AutoDock tool was used to set the grid box for docking simulations. In addition, the docking protocol was validated by extracting and re-docking the co-crystallized ligand into the active site (Fig. 5). Next, potent compounds and reference drug GEF were docked with the target to determine the docking parameters with the help of grid-based ligand docking (center_x = 1.45748, center_y = 194.208, center_z = 20.4128 and size_x = 30, size_y = 30, size_z = 30). Finally, the interaction information and the pictorial representation of the interaction between the ligands and the target were processed using Discovery Studio 2021 software.[35]

4. Conclusion

In summary, twenty 3-methylenamino-4(3*H*)-quinazolone derivatives have been designed, synthesized, and screened for anticancer activity as well as molecular docking and *in silico* ADMET studies. These derivatives were synthesized with good yields (66–90%) in a short time (1–2 h) using the classical reflux method. Additionally, *in vitro* results demonstrated that compound **5** exhibited good cytotoxic activity against the RD cell line (IC_{50} = 14.65 μM), while compounds **6** and **7** showed good cytotoxic activity against the MDA-MB-231 cell line with IC_{50} values of 10.62 and 8.79 μM, respectively. In particular, these compounds exhibited weak cytotoxic activity against the LLC-PK1 normal cell line compared to paclitaxel. This result demonstrated their selective anticancer properties. Furthermore, molecular docking predicted that compounds **5**, **6**, and **7** showed a strong binding affinity from −9.6 kcal mol^{-1} to −10.1 kcal mol^{-1} with the crucial residue of the EGFR target that resembles the co-crystallization ligand and reference drug Gefitinib. The obtained *in silico* ADMET results suggested that these potent derivatives possess a good ADMET profile. This work paved the way for the synthesis of more potent compounds based on 3-methyleneamino-4(3*H*)-quinazolone scaffolds and explored their various biological activities as well as their mechanism of action.

Author contributions

Tuyen Ngoc Truong: conceptualization, methodology, investigation, data curation, supervision, writing-original draft preparation. Em Canh Pham: methodology, investigation, writing-original draft preparation. Ngoc Vi Nguyen Tran: investigation. Phu Thien Tieu: investigation. My Hanh Thi Cao: investigation. Hong Tuoi Thi Do: investigation, supervision. Khanh N. B. Le: data curation, supervision, writing-original draft preparation, writing – review & editing.

Conflicts of interest

The authors declare that they have no known competing financial interests or personal relationships that could have appeared to influence the work reported in this paper.

Data availability

Software used in paper: molecular docking software: AutoDock Vina v1.2.x, URL: **https://vina.scripps.edu/**. ADMET software: ADMETlab3.0, URL: **https://admetlab3.scbdd.com/**. Target (Protein Data Bank): URL: **https://www.rcsb.org**.

IR, MS, and NMR spectra. See DOI: **https://doi.org/10.1039/d5ra03933a**.

Acknowledgements

This research was funded by the University of Medicine and Pharmacy at Ho Chi Minh City under contract number 06/2024/HĐ-ĐHYD, dated 29/3/2024.

References

1 P. S. Auti, G. George and A. T. Paul, *RSC Adv.*, 2020, **10**, 41353–41392.
2 F. Plescia, B. Maggio, G. Daidone and D. Raffa, *Eur. J. Med. Chem.*, 2021, **213**, 113070.
3 P. C. Em, L. T. Tuong Vi, L. H. Huong Ha, V. T. Bich Ngoc, B. V. Long, V. T. Thao, D. V. Duy, T. N. Ngoc Vi, N. L. Bao Khanh and N. T. Tuyen, *RSC Adv.*, 2023, **13**, 399–420.
4 P. C. Em and N. T. Tuyen, *ACS Omega*, 2022, **7**, 33614–33628.
5 P. C. Em, L. T. Tuong Vi, T. P. Long, T. N. Huong-Giang, N. L. Bao Khanh and N. T. Tuyen, *Arabian J. Chem.*, 2022, **15**, 103682.
6 S. I. Qureshi and H. K. Chaudhari, *Bioorg. Med. Chem.*, 2019, **27**, 2676–2688.
7 R. Bouley, D. Ding, Z. Peng, M. Bastian, E. Lastochkin, W. Song, M. A. Suckow, V. A. Schroeder, W. R. Wolter, S. Mobashery and M. Chang, *J. Med. Chem.*, 2016, **59**, 5011–5021.
8 S. Gatadi, J. Gour, M. Shukla, G. Kaul, S. Das, A. Dasgupta, S. Malasala, R. S. Borra, Y. V. Madhavi, S. Chopra and S. Nanduri, *Eur. J. Med. Chem.*, 2018, **157**, 1056–1067.
9 H. T. Tran, O. N. T. Vu, T. N. T. Le, B. D. C. Nguyen and N. N. Vo, *Appl. Sci.*, 2022, **12**, 2710.
10 N. B. Patel and J. C. Patel, *Arabian J. Chem.*, 2011, **4**, 403–411.

11 M. F. Zayed, H. E. A. Ahmed, S. Ihmaid, A. M. Omar and A. S. Abdelrahim, *J. Taibah Univ. Med. Sci.*, 2015, **10**, 333e339.
12 R. S. Gouhar, D. S. A. Haneen and S. M. El-Hallouty, *J. Heterocycl. Chem.*, 2019, **56**, 1651–1660.
13 N. N. E. El-Sayed, N. M. Almaneai, A. Ben Bacha, O. Al-Obeed, R. Ahmad, M. Abdulla and A. M. Alafeefy, *J. Enzyme Inhib. Med. Chem.*, 2019, **34**, 672–683.
14 Y. Riadi, M. A. Alamri, M. H. Geesi, E. H. Anouar, O. Ouerghi, A. B. Alabbas, M. A. Alossaimi, A. Altharawi, O. Dehbi and S. M. Alqahtani, *J. Biomol. Struct. Dyn.*, 2022, **40**, 6810–6816.
15 N. N. E. El-Sayed, T. M. Al-Otaibi, M. Alonazi, V. H. Masand, A. Barakat, Z. M. Almarhoon and A. Ben Bacha, *Molecules*, 2021, **26**, 3121.
16 K. Hemalatha and K. Girija, *Int. J. Pharm. Pharm. Sci.*, 2011, **3**, 103–106.
17 M. M. Aly, Y. A. Mohamed, K. A. M. El-Bayouki, W. M. Basyouni and S. Y. Abbas, *Eur. J. Med. Chem.*, 2010, **45**, 3365–3373.
18 V. Alagarsamy, V. Raja Solomon and K. Dhanabal, *Bioorg. Med. Chem.*, 2007, **15**, 235–241.
19 S. K. Krishnan, S. Ganguly, R. Veerasamy and B. Jan, *Eur. Rev. Med. Pharmacol. Sci.*, 2011, **15**, 673–681.
20 K. S. Kumar, S. Ganguly, R. Veerasamy and E. De Clercq, *Eur. J. Med. Chem.*, 2010, **45**, 5474–5479.
21 P. Nandy, M. T. Vishalakshi and A. R. Bhat, *Indian J. Heterocycl. Chem.*, 2006, **15**, 293–294.
22 G. Saravanan, V. Alagarsamy and C. R. Prakash, *Int. J. Pharm. Pharm. Sci.*, 2010, **2**, 83–86.
23 T. Mohamed and P. P. N. Rao, *Eur. J. Med. Chem.*, 2017, **26**, 823–843.
24 V. Alagarsamy and U. S. Pathak, *Bioorg. Med. Chem.*, 2007, **15**, 3457–3462.
25 P. P. Ding, M. Gao, B. B. Mao, S. L. Cao, C. H. Liu, C. R. Yang, Z. F. Li, J. Liao, H. Zhao, Z. Li, J. Li, H. Wang and X. Xu, *Eur. J. Med. Chem.*, 2016, **108**, 364–373.
26 C. J. Wang, X. Guo, R. Q. Zhai, C. Sun, G. Xiao, J. Chen, M. Y. Wei, C. L. Shao and Y. Gu, *Eur. J. Med. Chem.*, 2021, **224**, 113671.
27 M. M. Saleh Al Ward, A. E. Abdallah, M. F. Zayed, R. R. Ayyad, T. M. Abdelghany, D. A. Bakhotmah and M. A. El-Zahabi, *Future Med. Chem.*, 2024, **16**, 2523–2533.
28 F. Hakim, R. Salfi, D. Bhikshapathi and A. Khan, *Adv. Anticancer Agents Med. Chem.*, 2022, **22**, 926–932.
29 W. Dohle, F. L. Jourdan, G. Menchon, A. E. Prota, P. A. Foster, P. Mannion, E. Hamel, M. P. Thomas, P. G. Kasprzyk, E. Ferrandis, M. O. Steinmetz, M. P. Leese and B. V. L. Potter, *J. Med. Chem.*, 2018, **61**, 1031–1044.
30 E. O. Osman, S. H. Emam, A. Sonousi, M. M. Kandil, A. M. Abdou and R. A. Hassan, *Drug Dev. Res.*, 2023, **84**, 888–906.
31 M. Mortazavi, M. Divar, T. Damghani, F. Moosavi, L. Saso, S. Pirhadi, M. Khoshneviszadeh, N. Edraki and O. Firuzi, *Front. Chem.*, 2022, **10**, 969559.
32 Y. M. Khetmalis, A. Fathima, M. Schweipert, C. Debarnot, N. V. M. R. Bandaru, S. Murugesan, T. Jamma, F. J. Meyer-Almes and K. V. G. C. Sekhar, *Int. J. Mol. Sci.*, 2023, **24**, 11044.
33 K. Haider, S. Das, A. Joseph and M. S. Yar, *Drug Dev. Res.*, 2022, **83**, 859–890.
34 A. M. Emam, A. Dahal, S. S. Singh, R. D. Tosso, S. M. Ibrahim, M. El-Sadek, S. D. Jois, R. D. Enriz and H. Kothayer, *Arch. Pharm.*, 2021, **354**, e2100281.
35 P. C. Em, L. T. Tuong Vi and N. T. Tuyen, *RSC Adv.*, 2022, **12**, 21621–21646.
36 P. C. Em, N. T. Tuyen, D. Hanh Nguyen, D. V. Duy and D. T. Hong Tuoi, *Med. Chem.*, 2022, **18**, 558–573.
37 L. Fu, S. Shi, J. Yi, N. Wang, Y. He, Z. Wu, J. Peng, Y. Deng, W. Wang, C. Wu, A. Lyu, X. Zeng, W. Zhao, T. Hou and D. Cao, *Nucleic Acids Res.*, 2024, **52**, W422–W431.